

Rest-wavelength fiducials for the ITER core imaging x-ray spectrometer

P. Beiersdorfer, G. V. Brown, A. T. Graf, M. Bitter, K. W. Hill et al.

Citation: *Rev. Sci. Instrum.* **83**, 10E111 (2012); doi: 10.1063/1.4733318

View online: <http://dx.doi.org/10.1063/1.4733318>

View Table of Contents: <http://rsi.aip.org/resource/1/RSINAK/v83/i10>

Published by the [American Institute of Physics](#).

Related Articles

A setup for resonant inelastic soft x-ray scattering on liquids at free electron laser light sources

Rev. Sci. Instrum. **83**, 123109 (2012)

Obtaining material identification with cosmic ray radiography

AIP Advances **2**, 042128 (2012)

X-ray luminescence based spectrometer for investigation of scintillation properties

Rev. Sci. Instrum. **83**, 103112 (2012)

Developing small vacuum spark as an x-ray source for calibration of an x-ray focusing crystal spectrometer

Rev. Sci. Instrum. **83**, 103110 (2012)

A von Hamos x-ray spectrometer based on a segmented-type diffraction crystal for single-shot x-ray emission spectroscopy and time-resolved resonant inelastic x-ray scattering studies

Rev. Sci. Instrum. **83**, 103105 (2012)

Additional information on *Rev. Sci. Instrum.*


Journal Homepage: <http://rsi.aip.org>

Journal Information: http://rsi.aip.org/about/about_the_journal

Top downloads: http://rsi.aip.org/features/most_downloaded


Information for Authors: <http://rsi.aip.org/authors>

ADVERTISEMENT



JANIS

Does your research require low temperatures? Contact Janis today.
Our engineers will assist you in choosing the best system for your application.



10 mK to 800 K
Cryocoolers
Dilution Refrigerator Systems
Micro-manipulated Probe Stations

LHe/LN₂ Cryostats
Magnet Systems

sales@janis.com www.janis.com
Click to view our product web page.

Rest-wavelength fiducials for the ITER core imaging x-ray spectrometer^{a)}

P. Beiersdorfer,^{1,2,b)} G. V. Brown,¹ A. T. Graf,¹ M. Bitter,³ K. W. Hill,³ R. L. Kelley,⁴
C. A. Kilbourne,⁴ M. A. Leutenegger,⁴ and F. S. Porter⁴

¹Physics Division, Lawrence Livermore National Laboratory, Livermore, California 94550, USA

²Department of Chemistry and Chemical Physics Program, University of Puerto Rico, San Juan, Puerto Rico 00931, USA

³Princeton Plasma Physics Laboratory, Princeton, New Jersey 08543, USA

⁴Goddard Space Flight Center, Greenbelt, Maryland 20771, USA

(Presented 9 May 2012; received 27 April 2012; accepted 13 June 2012;
published online 12 July 2012)

Absolute wavelength references are needed to derive the plasma velocities from the Doppler shift of a given line emitted by a moving plasma. We show that such reference standards exist for the strongest x-ray line in neonlike W^{64+} , which has become the line of choice for the ITER (Latin “the way”) core imaging x-ray spectrometer. Close-by standards are the Hf $L\beta_3$ line and the Ir $L\alpha_2$ line, which bracket the W^{64+} line by ± 30 eV; other standards are given by the Ir $L\alpha_1$ and $L\alpha_2$ lines and the Hf $L\beta_1$ and $L\beta_2$ lines, which bracket the W^{64+} line by ± 40 and ± 160 eV, respectively. The reference standards can be produced by an x-ray tube built into the ITER spectrometer. We present spectra of the reference lines obtained with an x-ray microcalorimeter and compare them to spectra of the W^{64+} line obtained both with an x-ray microcalorimeter and a crystal spectrometer. © 2012 American Institute of Physics. [<http://dx.doi.org/10.1063/1.4733318>]

I. INTRODUCTION

Because of the sheer size of the ITER (Latin “the way”) plasma, plasma rotation will be measured using passive x-ray spectroscopy, which can readily observe core plasma, instead of using active neutral beam probes, which have difficulties penetrating to the core. Passive x-ray spectroscopy has been successfully used on various tokamaks, including the Tokamak Fusion Test Reactor (TFTR) and Alcator C-mod,^{1,2} to measure the bulk plasma rotation velocity, and thus it is a well tested, reliable method.

In a spectroscopic measurement, bulk plasma motion is inferred from the observed line shift $\Delta\lambda = \lambda - \lambda_0$ where λ is the measured position of the x-ray line, and λ_0 is its rest wavelength. This shift is proportional to the plasma rotation velocity v_ϕ by the expression

$$\Delta\lambda = (\lambda_0/c)v_\phi \cos \alpha, \quad (1)$$

where c is the speed of light, and α is the angle of intersection between the line of sight of the spectrometer and velocity vector on a given flux surface. We note that α varies along the line of sight so that the shift varies and causes some degree of line broadening that adds to the thermal broadening of the line. Similar to the effect caused by crystal focusing errors,³ this effect needs to be taken into account in the analysis.

The development of imaging crystal spectrometers^{4,5} has now made it possible to produce radial profiles of the plasma

rotation using tomographic imaging techniques.⁶ The core imaging x-ray spectrometer (CIXS) is a diagnostic designed to make use of an imaging geometry to measure the ion temperature and bulk rotation velocity of the core plasma.⁷ The CIXS has been designed to focus on the strongest x-ray line from neonlike tungsten, W^{64+} , which is situated near 9126 eV.⁸ Tungsten has the advantage that it is an intrinsic plasma impurity of ITER. But it can also be injected as a solid or gas, if needed. For example, tungsten was injected using laser blow-off on Alcator,⁹ powder injection on the National Spherical Torus Experiment (NSTX),¹⁰ and via gas injection, employing tungsten hexacarbonyl on the Sustained Spheromak Physics Experiment (SSPX).¹¹ Plasma rotation at the levels of 500 km/s seen in TFTR, for example, see Ref. 12, would shift the line on the order of 10 eV or less, depending on the value of α .

A major issue with a spectroscopic determination of the rotation velocity is the lack of an absolute x-ray wavelength calibration, causing an arbitrary offset of the velocity values. In other words, the line may already be shifted from the first moment it is detected, and any subsequent shifts only add or subtract from the initial level of unknown magnitude. In the following, we address this problem by suggesting the use of characteristic x-ray lines produced inside the spectrometer either by an x-ray tube or by fluorescence to provide an absolute calibration.

II. X-RAY REFERENCE STANDARDS

There are numerous characteristic x-ray lines from the naturally occurring elements, which can serve as reference lines.¹³ However, they are spaced rather far apart in some energy regions so that it is not always possible to find suitable lines. In the vicinity of the W^{64+} line, commonly referred to

^{a)}Contributed paper, published as part of the Proceedings of the 19th Topical Conference on High-Temperature Plasma Diagnostics, Monterey, California, May 2012.

^{b)}Author to whom correspondence should be addressed: beiersdorfer@llnl.gov.

TABLE I. X-ray lines within ± 250 eV of the neonlike W^{64+} line 3D according to Ref. 12.

Element label	Transition		Energy (eV)
Hf	$L\beta_4$	$L_I M_{II}$	8905.4
Hf	$L\beta_1$	$L_{II} M_{IV}$	9022.7
Hf	$L\beta_3$	$L_I M_{III}$	9163.4
Hf	$L\beta_2$	$L_{III} M_V$	9347.3
Ir	$L\alpha_2$	$L_{III} M_{IV}$	9099.5
Ir	$L\alpha_1$	$L_{III} M_V$	9175.1

as line 3D, there are several candidate reference lines from Hf and Ir, as summarized in Table I.

We have measured the x-ray spectrum from both Hf and Ir, photofluoresced using an x-ray tube with a tungsten anode. Photofluorescing the Hf and Ir targets produces pure characteristic lines without the associated Bremsstrahlung background produced using electron impact. The tube was operated at a voltage of 20 kV and a current of $1 \mu A$. The emitted x rays were recorded with a flight-spares x-ray microcalorimeter produced for the Astro-H x-ray observatory at the Goddard Space Flight Center.¹⁴ This device is similar to the EBIT calorimeter spectrometer used at the Livermore electron beam ion trap¹⁵ and can be used on ITER for ion temperature measurements to augment the capabilities of the CIXS.¹⁶

The measured spectrum of Hf is shown in Fig. 1(a). The spectrum shows the four lines listed in Table I. We note that two lines— $L\beta_1$ and $L\beta_2$ —are strong, while the other two are weak. In particular, the $L\beta_1$, which is the strongest of the four lines, is about ten times more intense than the $L\beta_3$ line, while the $L\beta_2$ line is about five times stronger than $L\beta_3$.

In Fig. 1(b), we show the measured spectrum of the Ir $L\alpha_1$ and $L\alpha_2$ lines. As seen from the figure, the $L\alpha_1$ is an order of magnitude more intense than the α_2 line.

The Hf and Ir spectra can be compared to the spectrum of highly charged tungsten produced on the Livermore SuperEBIT electron beam ion trap shown in Fig. 1(c).^{17,18} This spectrum was recorded using an electron beam energy of 23 keV and shows the 3D line and several collisional satellite lines from lower and higher neighboring charge states.

The original CIXS design envisioned the use of a Pilatus-II-type detector placed about 1 m away from the crystal. In this case, the detector records x rays in a range spanning about 450 eV centered around the 3D line.⁷ However, the extent of the observable x-ray range depends also on the width of the aperture within the hard x-ray and neutron shield. This likely needs to be minimized to reduce the amount of irradiation of other instruments in the ITER port plug that are co-located with the CIXS. As a result, only the central part of the detector will record the x-ray spectrum from ITER, and the outer parts can be used to record the reference lines. The two strong Hf $L\beta_1$ and Hf $L\beta_2$ lines at 9022.7 and 9347.3 eV (cf. Table I) bracket the 3D line and are excellent candidates to serve as x-ray standards.

In order to provide for more room for co-located diagnostics, there is the possibility of shrinking the size of the crystal spectrometer by about 80% of the original size and, most importantly, to utilize smaller detectors. In this case, the en-

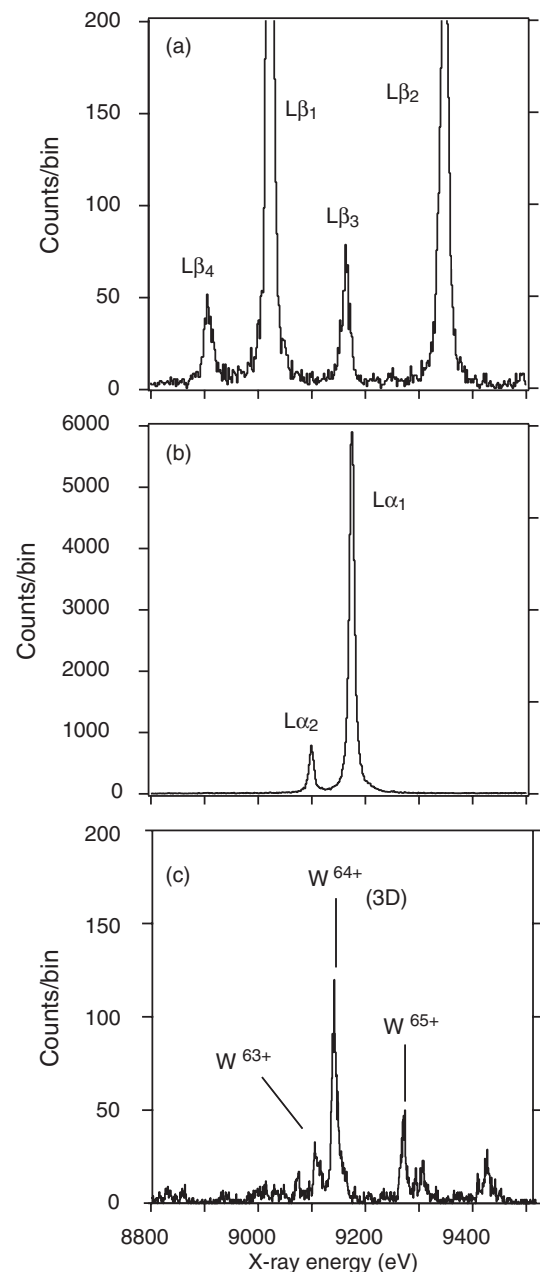


FIG. 1. X-ray spectra in the working range of the ITER CIXS diagnostic: (a) characteristic x-ray lines from Hf; (b) characteristic x-ray lines from Ir; (c) W^{64+} line and neighboring inner-shell collisional satellite lines. The spectra were recorded using an x-ray microcalorimeter with a resolution of 4.5 eV at 6 keV and 5 eV at 9 keV FWHM.

ergy range covered by the detector may shrink considerably, and the reference standards may have to be closer to line 3D. We propose to utilize the Ir $L\alpha_1$ and $L\alpha_2$ lines at 9099.5 and 9175.1 eV, respectively, to bracket the 3D line. These lines are only 76 eV apart and are a perfect pair for calibrating a narrow detector. An even closer bracket can be achieved by utilizing lines from both Ir and Hf, i.e., the Ir $L\alpha_1$ line at 9099.5 eV and the $L\beta_3$ line at 9163.4 eV (cf. Table I). These two lines are only 64 eV apart. However, the Hf line is much weaker than the Ir line, and thus this pair is more difficult to implement. Moreover, the tail of one of the reference lines may overlap

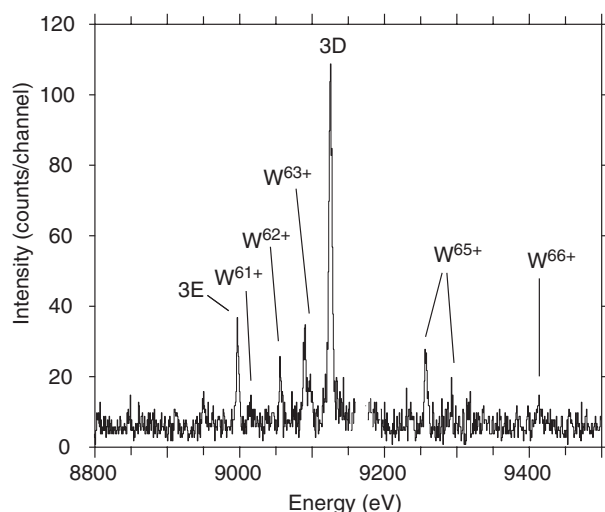


FIG. 2. X-ray spectrum of the W^{64+} 3D line and neighboring innershell collisional satellite lines observed with a crystal spectrometer on the Livermore electron beam ion trap. The gap in the middle of the spectrum is where a fiducial line was used to track electronic drifts.

with the tungsten line, especially if the tungsten line shifts as much as 10 eV.

We point out that two reference lines are, in principle, not needed for an absolute energy calibration of the CIXS; one is sufficient to anchor the absolute wavelength scale. The second line gives the spectral dispersion. The x-ray spectrum of tungsten near the 3D line has several other lines that can be used to establish the dispersion, if their wavelengths are known with sufficient accuracy. This assumes that the neighboring lines are emitted from plasma with the same rotation velocity. Having the second reference line, however, allows us to check for differential changes in plasma rotation and thus is important to have.

The lines from highly charged tungsten are known from theoretical calculations, which may not provide the accuracy needed for establishing a reliable dispersion. However, high-resolution measurements using crystal spectrometers have now been performed on the Livermore electron beam ion trap, providing experimental transition energies with an accuracy of about ± 0.5 eV.⁸ A spectrum of the vicinity of the 3D line from those experiments is shown in Fig. 2. The energy of the 3D line determined in these measurements is 9126.25 ± 0.50 eV.⁸

III. FURTHER ISSUES

Characteristic x-ray lines are inherently broad. In part, this is because the radiative rates of the transitions comprising these lines are typically larger than the corresponding transitions in highly charged ions. But, the main reason is that these transitions have a large number of spectator electrons, and a given characteristic x-ray line (which should better be referred to as a ‘feature’) consists of a covey of transitions (see, for example, Deutsch *et al.*¹⁹).

The tungsten 3D lines have a width of about 5.5 eV at an ion temperature of 10 keV and about 8.5 eV at 25 keV. The Ir $L\alpha_1$ line has a width comparable to, albeit slightly larger

than that of tungsten at 25 keV (we measure roughly 9 eV). Based on the design presented in Ref. 7, the CIXS will count about 10,000 counts in line 3D per millisecond, if the plasma temperature is 25 keV and the tungsten concentration is 10^{-5} . This means that the position of the 3D line will be determined within an accuracy of about 10^{-5} Å, i.e., similar to what was achieved on TFTR.¹ In order to determine the position of the Ir line to within one part in 10^5 , i.e., to within 100th of the line width or about 10^{-5} Å, one also roughly needs 10 000 counts. This sets a limit on what flux of characteristic x rays will be needed in order to perform the calibration at a specific time resolution.

ACKNOWLEDGMENTS

This work was performed under the auspices of the DOE by LLNL under Contract No. DE-AC52-07NA27344. P.B. would like to thank Prof. Y. Ishikawa and the University of Puerto Rico for their hospitality during the preparation of this manuscript.

- ¹M. Bitter, K. L. Wong, S. Scott, H. Hsuan, B. Grek, D. Johnson, and G. Tait, *Phys. Fluids B* **2**, 1503 (1990).
- ²J. E. Rice, J. A. Goetz, R. S. Granetz, M. J. Greenwald, A. E. Hubbard, L. H. Hutchinson, E. S. Marmor, D. Mossessian, T. S. Pedersen, J. A. Snipes, J. L. Terry, and S. M. Wolfe, *Phys. Plasmas* **7**, 1825 (2000).
- ³E. Wang, P. Beiersdorfer, M. Gu, M. Bitter, L. Delgado-Aparicio, K. W. Hill, M. Reinke, J. E. Rice, and Y. Podpaly, *Rev. Sci. Instrum.* **81**, 10E329 (2010).
- ⁴M. Bitter, K. W. Hill, A. L. Roquemore, P. Beiersdorfer, S. M. Kahn, S. R. Elliott, and B. Fraenkel, *Rev. Sci. Instrum.* **70**, 292 (1999).
- ⁵M. Bitter, K. W. Hill, B. Stratton, A. L. Roquemore, D. Mastrovito, S. G. Lee, J. G. Bak, M. K. Moon, U. W. Nam, G. Smith, J. E. Rice, P. Beiersdorfer, and B. S. Fraenkel, *Rev. Sci. Instrum.* **75**, 3660 (2004).
- ⁶K. W. Hill, M. L. Bitter, S. D. Scott, A. Ince-Cushman, M. Reinke, J. E. Rice, P. Beiersdorfer, M.-F. Gu, S. G. Lee, Ch. Broennimann, and E. F. Eikenberry, *Rev. Sci. Instrum.* **79**, 10E320 (2008).
- ⁷P. Beiersdorfer, J. Clementson, J. Dunn, M. F. Gu, K. Morris, Y. Podpaly, E. Wang, M. Bitter, R. Feder, K. W. Hill, D. Johnson, and R. Barnsley, *J. Phys. B* **43**, 144008 (2010).
- ⁸P. Beiersdorfer, J. K. Lepson, M. B. Schneider, and M. P. Bode, “L-shell x-ray emission from neonlike W_{64+} ,” *Phys. Rev. A* (in press).
- ⁹M. L. Reinke, P. Beiersdorfer, N. T. Howard, E. W. Magee, Y. Podpaly, J. E. Rice, and J. L. Terry, *Rev. Sci. Instrum.* **81**, 10D736 (2010).
- ¹⁰J. Clementson, P. Beiersdorfer, A. L. Roquemore, C. H. Skinner, D. K. Mansfield, K. Hartzfeld, and J. K. Lepson, *Rev. Sci. Instrum.* **81**, 10E326 (2010).
- ¹¹J. Clementson, P. Beiersdorfer, E. W. Magee, H. S. McLean, and W. D. Wood, *J. Phys. B* **43**, 144009 (2010).
- ¹²M. Bitter, H. Hsuan, J. E. Rice, K. W. Hill, M. Diesso, B. Grek, R. Hulse, D. W. Johnson, L. C. Johnson, and S. von Goeler, *Rev. Sci. Instrum.* **59**, 2131 (1988).
- ¹³J. Bearden, *Rev. Mod. Phys.* **39**, 78 (1967).
- ¹⁴F. S. Porter, J. S. Adams, G. V. Brown, J. A. Chervenak, M. P. Chiao, R. Fujimoto, Y. Ishisaki, R. L. Kelley, C. A. Kilbourne, D. McCammon, K. Mitsuda, T. Ohashi, A. E. Szymkowiak, Y. Takei, M. Tashiro, and N. Yamasaki, *Proc. SPIE* **7732**, 77323J (2010).
- ¹⁵F. S. Porter, B. R. Beck, P. Beiersdorfer, K. R. Boyce, G. V. Brown, H. Chen, J. Gygas, S. M. Kahn, R. L. Kelley, C. A. Kilbourne, E. Magee, and D. B. Thorn, *Can. J. Phys.* **86**, 231 (2008).
- ¹⁶P. Beiersdorfer, G. V. Brown, J. Clementson, J. Dunn, M. F. Gu, K. Morris, E. Wang, R. L. Kelley, C. A. Kilbourne, F. S. Porter, M. Bitter, R. Feder, K. W. Hill, D. Johnson, and R. Barnsley, *Rev. Sci. Instrum.* **81**, 10E323 (2010).
- ¹⁷R. E. Marrs, P. Beiersdorfer, and D. Schneider, *Phys. Today* **47**, 27 (1994).
- ¹⁸P. Beiersdorfer, *Can. J. Phys.* **86**, 1 (2008).
- ¹⁹M. Deutsch, E. Förster, G. Hölzer, J. Härtwig, K. Hämäläinen, C. Kao, S. Huotari, and R. Diamant, *J. Res. Natl. Inst. Stand. Technol.* **109**, 75 (2004).